Scaling quantum-dot light-emitting diodes to submicrometer sizes

A. Fiore[a)]
Institute of Quantum Electronics and Photonics, Ecole Polytechnique Fédérale de Lausanne, CH-1015 Lausanne, Switzerland and Institute of Photonics and Nanotechnology, CNR, via del Cineto Romano 42, 00156 Roma, Italy

J. X. Chen[b)] and M. Ilegems
Institute of Quantum Electronics and Photonics, Ecole Polytechnique Fédérale de Lausanne, CH-1015 Lausanne, Switzerland

(Received 2 May 2002; accepted for publication 10 July 2002)

We introduce a device structure and a fabrication technique that allow the realization of efficient light-emitting diodes (LEDs) with dimensions of the active area in the ≈ 100 nm range. Using optical lithography, selective oxidation, and an active region consisting of InAs quantum dots (QDs), we fabricated LEDs with light–current–voltage characteristics which scale well with nominal device area down to 600 nm diam at room temperature. The scaling behavior provides evidence for strong carrier confinement in the QDs and shows the potential for the realization of high-efficiency single-photon LEDs operating at room temperature. © *2002 American Institute of Physics.* [DOI: 10.1063/1.1504880]

Device size scaling is the subject of major research interest, in optoelectronics as in electronics. For some applications, high efficiency from a light-emitting device (laser, LED) is needed at low current levels. Since high efficiency is usually reached at a given current density, this requires reducing the device area, i.e., scaling down the device. Moreover, efficient coupling to single-mode fibers requires small active areas (in the few micrometer range). Examples of scaling issues are found in edge-emitting lasers for optical communication in single-mode fibers, 980 nm pump lasers for fiber amplifiers, and low-threshold vertical-cavity surface-emitting lasers (VCSELs). Recently, a further stimulus towards the realization of ultrasmall optical devices is coming from the field of quantum communication and quantum computing based on semiconductor nanostructures. As an example, efficient and compact single-photon emitters might be realized from single semiconductor quantum dots (QDs),[1–4] if a way is found to isolate and efficiently inject current into a single QD. While antibunching in electrically pumped single QDs has been very recently demonstrated,[5] the device structure adopted in that case, which is based on postfiltering of emitted photons rather than selective injection, is not suitable for a high-efficiency single-photon emitter. If the active material is constituted by self-assembled QDs, which typically have areal densities in the 10^8-10^{11} cm^{-2} range, the active device size should be well below 1 μm in order to contain a single QD, which represents a formidable task for both device design and fabrication. Three major problems are faced when one tries to scale down the device size while keeping good efficiency. First, if etching through the active region is used to define the active area, nonradiative recombination at etched sidewalls strongly reduces the efficiency as the perimeter/area ratio increases. Second, if a current-blocking layer is used to define a current aperture near the active region (e.g., Al_2O_3 obtained by selective oxidation of AlGaAs in VCSELs), current spreading between the blocking layer and the active region can increase the effective active diameter by several micrometers.[6–8] Finally, carrier diffusion in the active region [usually quantum wells (QWs)] increases the effective radius by the diffusion length, typically, 1–2 μm. While current spreading can be minimized by proper design of the injection region, carrier diffusion can be suppressed only by applying a lateral carrier confinement in the active region. Several approaches have been reported, such as QW interdiffusion,[9] segmented QWs,[10] and self-assembled QDs,[11] although with limited success, probably due to the need to combine strong carrier confinement and good radiative properties of the active material.

In this letter, we propose an approach to the realization of ultrasmall light-emitting devices with active areas well below 1 μm^2, which relies on three points: (a) Fabrication of current apertures in the ≈ 100 nm range using standard optical lithography, selective oxidation of AlGaAs and self-aligned contact definition; (b) optimized current injection in the active region using a graded-band-gap hole injector; and (c) suppression of lateral carrier diffusion by the use of self-assembled QDs with deep three-dimensional (3D) confinement potential. Using this approach, we demonstrate QD LEDs with characteristics that scale well with nominal size down to 600 nm at room temperature (RT), showing that lateral current spreading and carrier diffusion are effectively suppressed even at RT. This could open the way to high-performance, ultrasmall QD-based LEDs and VCSELs, and ultimately high-efficiency single-photon LEDs.

Bottom-emitting microcavity LEDs with a single layer of self-assembled QDs were grown by molecular beam epitaxy on n-doped (001) GaAs substrates [see the sketch in Fig. 1(a)]. The bottom mirror consists of a 3.5 period n-doped GaAs/$Al_{0.9}Ga_{0.1}As$ quarter-wave stack. The cavity is made of 20 nm n-$Al_{0.3}Ga_{0.7}As$, 114 nm n-GaAs, 45 nm

a)Electronic mail: andrea.fiore@epfl.ch
b)Present address: Bell Laboratories, Lucent Technologies, Inc., 600 Mountain Ave., Murray Hill, NJ 07974.

 © 2002 American Institute of Physics

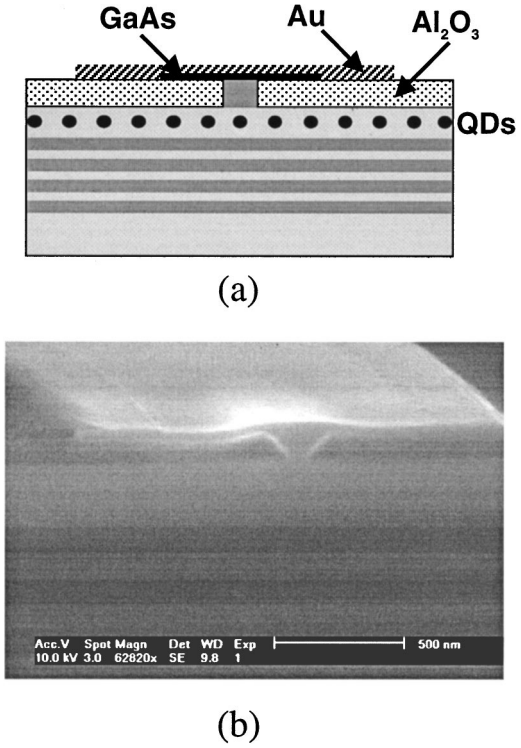

FIG. 1. (a) Schematics of the fabricated LED structure. (b) Cross-sectional SEM image of a 70 nm aperture obtained by lateral oxidation from a 1-μm-wide stripe.

undoped GaAs, a layer of QDs, and 45 nm undoped GaAs. The QDs are grown by continuously depositing 2.9 ML of InAs and covering with a 5-nm-thick $In_{0.15}Ga_{0.85}As$ layer to redshift the emission to the 1.3 μm region. These growth conditions produce QDs with 25 nm diam and 7 nm height, providing a strong RT photoluminescence peak at 1300 nm, with a full width at half maximum (FWHM) = 45 nm.[12] As compared to short-wavelength ($\approx$1000 nm) QDs, these dots have a larger potential barrier to carrier escape from the dot ground state to the wetting layer [the difference in transition energies is $\approx$300 meV (Ref. 13) as compared to $\approx$100 meV for short-wavelength QDs (Ref. 14)]. On top of the cavity, a hole injector is grown, consisting of a 32-nm-undoped graded-band-gap region with Al composition linearly increasing from 0% to 85%, and a 135 nm $Al_{0.85}Ga_{0.15}As$ current aperture to be oxidized. The bottom 20 nm in the $Al_{0.85}Ga_{0.15}As$ layer are undoped, while the rest is p doped ($p = 2\times10^{18}$ cm^{-3}). The structure is capped by a heavily doped GaAs p-contact layer. The injector is designed so as to facilitate vertical hole transport from the $Al_{0.85}Ga_{0.15}As$ aperture region to the QDs by avoiding potential steps at heterointerfaces in the valence band and by providing a potential gradient directed towards the active layer. The doping profile was also found to be critical.

Device processing starts with the definition of shallow mesas of variable diameter (1–30 μm) by optical lithography and wet etching of the top GaAs cap layer. The exposed $Al_{0.85}Ga_{0.15}As$ is then oxidized selectively by heating the sample at 400 °C for 55 min in a H_2O atmosphere created by bubbling N_2 in a water bath at 85 °C. The oxidation starts at the exposed surface and then penetrates laterally under the GaAs cap layer, thus defining a current aperture whose diameter can be controlled down to around 100 nm by varying

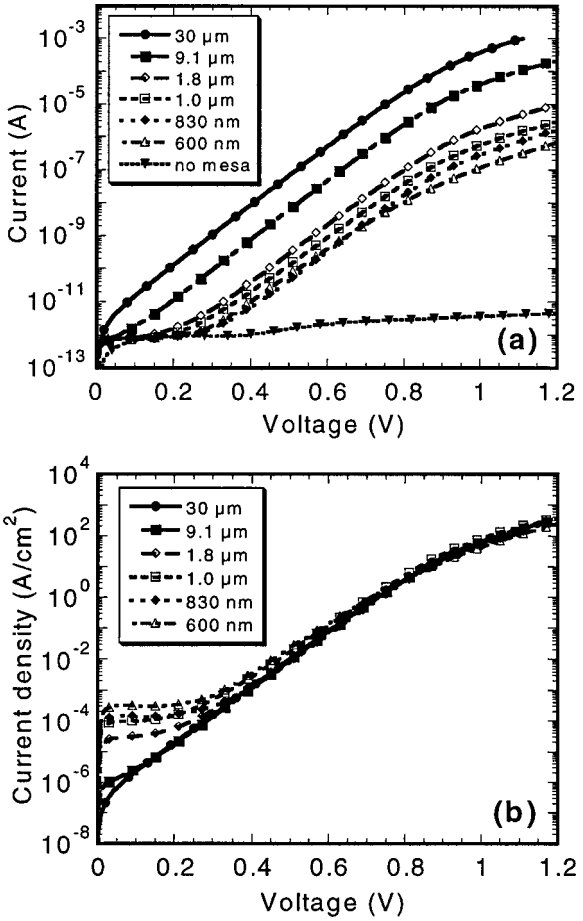

FIG. 2. (a) Room-temperature current–voltage characteristics of QD LEDs with current aperture diameters ranging from 30 μm to 600 nm ("no mesa:" control device with no current aperture). (b) Current density vs voltage curves for the same devices, calculated using the unoxidized aperture areas measured by SEM.

the oxidation time. Figure 1(b) shows a scanning-electron microscope (SEM) image of an aperture of 70 nm defined in this way. Broad-area p contacts (3.8×10^{-5} cm^2) are then evaporated on top of the mesas, with uncritical alignment, and an n contact is evaporated on the substrate side. Because the surface of the sample, outside of the mesas, is covered with an insulating Al_2O_3 oxide, current is forced to flow into the small current apertures. The key point which allows the definition of $\ll 1$ μm current apertures with such a simple procedure is the simultaneous and self-aligned definition of the current aperture and of a contact-defining oxide by means of the vertical–lateral oxidation of AlGaAs, as first proposed in Ref. 15. In contrast to previously reported approaches,[5,16] this allows us to fabricate devices with active diameters down to 100 nm by optical lithography.

Figure 2(a) shows the RT current versus voltage characteristics (measured in a two-probe setup) for current-aperture diameters ranging from 30 μm to 600 nm. The $I-V$ curve of a control device with no mesa (i.e., metal on oxide) is also shown for comparison. The curves can be fitted with the exponential diode characteristics (ideality factor $n\approx2$) over five to six orders of magnitude. At low bias ($V<0.3$ V), leakage through the broad-area oxide prevails over current flowing into the mesas for the smallest devices. Note that the leakage current density through the oxide is very low for the entire bias range investigated (maximum$\approx10^{-7}$ A/cm^2 at

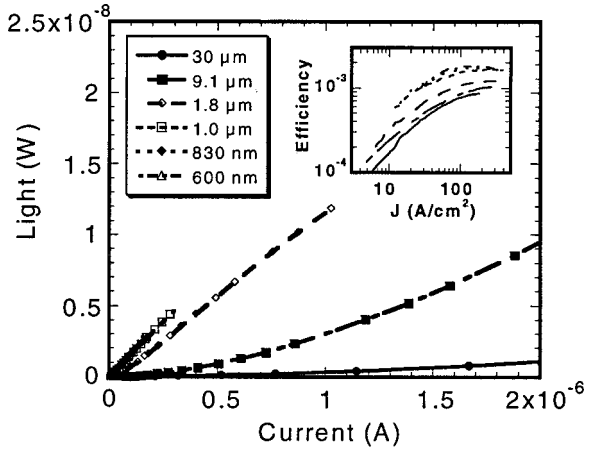

FIG. 3. Room-temperature light–current characteristics of QD LEDs. The $L-I$ curves of devices with diameters of 1.0 μm, 830 nm, and 600 nm are almost superposed, hence, hardly distinguishable. Inset: external quantum efficiency vs current density.

1.2 V). At high bias, the device resistance results in a departure from the ideal diode behavior. Figure 2(b) shows the current densities, calculated using the unoxidized aperture areas measured by SEM before evaporating the contacts, i.e., assuming no lateral carrier leakage. Remarkably, the curves superpose very well, particularly in the on-region of the diode ($V>0.6$ V). From the overlap among the different $J-V$ curves, we can estimate that the lateral diffusion/spreading length is well below 100 nm in the on-region. This proves that all carrier leakage paths (current spreading, carrier diffusion, and nonradiative recombination) are effectively suppressed in these structures. Some leakage is still seen at low bias (apparent current density larger for smaller devices, which implies an effective injection area larger than measured by SEM), which can be attributed to current spreading below the oxide at very high diode impedances.

In order to further confirm these conclusions, we investigated the efficiency in these ultrasmall LEDs. The light-current ($L-I$) characteristics at room temperature are shown in Fig. 3. In the low current range shown, large devices have very poor efficiency and nonlinear $L-I$ characteristics, which is an indication of predominant nonradiative recombination at very low current density, a common feature in LEDs. In contrast, small devices have linear $L-I$ curves and higher efficiency, because they operate at the optimum current density, which is around 100 A/cm^2 in this sample. It should be noticed that efficiency is not reduced even for the smallest devices of 600 nm diam. This proves that the oxide aperture does not introduce defects in the active region, which would systematically degrade the perfomance as the area is reduced. Also, by plotting the efficiency as a function of current density (inset of Fig. 3) we find good scaling behavior and similar peak efficiency for diameters ranging from 30 μm to 600 nm, which further confirm the negligible lateral carrier leakage. We found that the efficiency fluctuates considerably among nominally identical devices for diameters around and below 600 nm, some showing efficiencies even larger than broad-area devices (for this reason LEDs with diameters below 600 nm are not presented here). This may be attributed to growth-related nonradiative defects with areal density in the 10^8 cm^{-2} range, so that a small and variable number of them is present in the active area of submicrometer devices. The presence of defects is also confirmed by the relatively low peak external quantum efficiency of 0.1% measured in large (400 μm) devices, even with no oxide aperturing, as compared to efficiencies of over 1% measured by us[13] in similar QD structures.

In conclusion, we have presented an approach towards the scaling of light-emitting devices to submicrometer sizes. By combining a simple self-aligned fabrication technique with an optimized design of the epitaxial structure, it is possible to realize devices with active areas well below 1 μm^2 while keeping a constant efficiency. Scaling of $I-V$ and $L-I$ curves with nominal device area demonstrates that strong carrier 3D confinement in QDs results in a reduced diffusion length <100 nm even at room temperature. As it is clear from the light–current characteristics shown in Fig. 3, when low output powers are needed, small-scaled devices are more efficient than large devices which operate at much smaller current densities. The strong carrier confinement in QDs may be applied to the fabrication of submicrometer-sized lasers with ultrasmall threshold currents and of single-QD LEDs for single-photon applications.

The authors wish to thank Dr. R. P. Stanley (CSEM Neuchàtel) for many interesting discussions, and Professor C. Weisbuch (Ecole Polytechnique, Palaiseau) for stimulating this work. Financial support from the European Commission through the fifth framework IST program and from the Swiss National Science Foundation is acknowledged.

[1] O. Benson, C. Santori, M. Pelton, and Y. Yamamoto, Phys. Rev. Lett. **84**, 2513 (2000).
[2] P. Michler, A. Imamoglu, M. D. Mason, P. J. Carson, G. F. Strouse, and S. K. Buratto, Nature (London) **406**, 968 (2000).
[3] P. Michler, A. Kiraz, C. Becher, W. V. Schoenfeld, P. M. Petroff, L. Zhang, E. Hu, and A. Imamoglu, Science **290**, 2282 (2000).
[4] C. Santori, M. Pelton, G. Solomon, Y. Dale, and Y. Yamamoto, Phys. Rev. Lett. **86**, 1502 (2001).
[5] Z. Yuan, B. E. Kardynal, R. M. Stevenson, A. J. Shields, C. J. Lobo, K. Cooper, N. S. Beattie, D. A. Ritchie, and M. Pepper, Science **295**, 102 (2002).
[6] N. K. Dutta, J. Appl. Phys. **68**, 1961 (1990).
[7] G. M. Yang, M. H. MacDougal, and P. D. Dapkus, J. Appl. Phys. **80**, 4837 (1996).
[8] E. R. Hegblom, N. M. Margalit, A. Fiore, and L. A. Coldren, IEEE J. Sel. Top. Quantum Electron. **5**, 553 (1999).
[9] R. L. Naone, P. D. Floyd, D. B. Young, E. R. Hegblom, T. A. Strand, and L. A. Coldren, IEEE J. Sel. Top. Quantum Electron. **4**, 706 (1998).
[10] T. A. Strand, B. J. Thibeault, and L. A. Coldren, J. Appl. Phys. **81**, 3377 (1997).
[11] J. K. Kim, R. L. Naone, and L. A. Coldren, IEEE J. Sel. Top. Quantum Electron. **6**, 504 (2000).
[12] A. Fiore, U. Oesterle, R. P. Stanley, R. Houdré, F. Lelarge, M. Ilegems, P. Borri, W. Langbein, D. Birkedal, J. M. Hvam, M. Cantoni, and F. Bobard, IEEE J. Quantum Electron. **37**, 1050 (2001).
[13] A. Fiore, U. Oesterle, R. P. Stanley, and M. Ilegems, IEEE Photonics Technol. Lett. **12**, 1601 (2000).
[14] D. Bimberg, N. Kirstaedter, N. N. Ledentsov, Z. I. Alferov, P. S. Kop'ev, and V. M. Ustinov, IEEE J. Sel. Top. Quantum Electron. **3**, 196 (1997).
[15] F. A. Kish, S. J. Caracci, J. N. Holonyak, J. M. Dallesasse, K. C. Hsieh, S. C. Smith, and R. D. Burnham, Appl. Phys. Lett. **59**, 1755 (1991).
[16] H. Chen, Z. Zou, C. Cao, and D. G. Deppe, Appl. Phys. Lett. **80**, 350 (2002).